INTERNATIONAL JOURNAL OF CONSERVATION SCIENCE
ISSN: 2067-533X Volume 11, Issue 3, July-September 2020: 731-746 www.ijcs.ro

STUDY OF THE EFFECTS OF SKIN SURFACE LIPIDS ON OLD CELLULOSE-SUPPORT DOCUMENTS

Maria BOUTIUC (HAULICĂ)[1,2], Viorica VASILACHE[3*], Oana FLORESCU[1,4], Mihai BREBU[5], Ion SANDU[3,6], Petru Ovidiu TANASA[1], Ioan Cristinel NEGRU[1]

[1]„Al. I. Cuza" University of Iasi, Faculty of Geography and Geology, Doctoral School of Geosciences, 22 Carol I Blvd., 700506 Iasi, Romania
[2] County Service of the National Archives Iasi, Blvd. Carol I no. 26, 700505 Iaşi, Romania
[3]„Al. I. Cuza" University of Iasi, Institute of Interdisciplinary Research, ARHEOINVEST Centrum, 11 Carol I, Bld., 700506 Iasi, Romania
[4]„Poni – Cernatescu" Museum of Iasi, 7B Kogalniceanu St. 700454 Iasi, Romania
[5] Petru Poni Institute of Macromolecular Chemistry, 41A Aleea Grigore Ghica Vodă 700487 Iași, Romania
[6] Academy of Romanian Scientists (AOSR), 54 Splaiul Independentei St., Sect. 5, 050094 Bucharest, Romania

Abstract

The paper tackles the influence of skin surface lipids and chromatic fungal attack on the paper support and the writing of a 125-year-old document, which involves the corroboration between multianalytical techniques. Thus, the study used three specimens sampled from different areas: a standard lipid- and fungal-attack-free sample, one with old lipid film dating back to its being used by its creator (before it had entered the archives) and another with lipid film and fungal attack present on it (from after it had entered the archives). In addition to direct observation by means of magnifying instruments, our scientific research relied on the following techniques: OM, SEM-EDX, μ-FTIR and differential thermal analysis (TG, DTA and DTG). Compared to the standard sample, the data of which correspond to the natural aging process occurring between 1895 and 2020, the other two samples show evolutionary degradation effects under the influence of oxidatively fouled lipids and on small areas photochemically and thermally cornified, as well as effects due to enzymatic degradation under the influence of fungal attack. The study has a clear goal, namely to implement specific protection measures when dealing with old documents (gloves and protective mask, air conditioning niche for preservation-restoration actions).

Keywords*: Old documents; Cellulose support; Skin surface lipids; Fungal attack; OM; SEM-EDX; μ-FTIR; Thermal derivatography.*

Introduction

It is common knowledge that the anthropogenic factor (even authorized and qualified personnel for the use of documents, and also those who use them for scientific research) can negatively influence the state of preservation of archival documents and plays a significant role in their deterioration and degradation. Here are some of the most common causes: improper storage, improper handling, leafing through documents without wearing protective gloves (in latex or cotton), wetting one's fingers with saliva when browsing through them or talking over documents without wearing a protective mask. Following contact between the fingers and the document or when no protective mask is worn over the nose and mouth, skin surface lipids and saliva carbohydrates are deposited on the documents forming a greasy film, which over time

* Corresponding author: viorica_18v@yahoo.com

interacts strongly with the support, writing and drawing materials. These are generally human skin surface lipids, secreted by the sebaceous glands or resulting from the scaling of the superficial layer of corneocytes (the last stage of keratinocyte evolution) on the palm skin. Atmospheric dust and smog get stuck in this film, contaminating the cellulose support by catching dirt with microbial load [1].

Also, wetting one's fingers in one's mouth before browsing through the documents (before turning the pages) brings extra moisture, along with lipids, proteins, carbohydrates and dirt on the fingers, which become stuck on the page. Another undesirable situation for document preservation is that the user does not wear a simple mask or niche designed for dust removal and other important actions on the document. All these 'habits' create favorable conditions for the occurrence and proliferation of microorganisms.

The layer of lipids on the surface of the skin (fingers and palms) is 0.5 to 4 μm thick and consists of sebum secreted by the sebaceous glands and lipids surrounding cells in the *stratum corneum* (in the palm) [2] resulting from the desquamation of the superficial layer of corneocytes [3].

Sebum has a complex structure, consisting of diglycerides and triglycerides, and free fatty acids (50-60%), esterified waxes (20-30%), squalene (10-16%) and cholesterol esters (2-4%) [4, 5]. Triglycerides contain saturated and unsaturated fatty acids, with a single or branched chain, which can include up to 26 carbon atoms. Under the action of microbial enzymes (proteases) in the follicular duct, triglycerides are broken down into mono- and diglycerides, free fatty acids and glycerin [6]. The fatty acids in human sebum are the following organic acids: sapienic (16:1, Δ6); sabaleic (18:2, Δ5.8); lauric (C12:0); palmitic (C16:0) and oleic (C18:1, cis-9) [7, 8]. Wax esters are obtained from saturated or monounsaturated fatty acids (C12-C29), normal or branched, with fatty alcohols (C24-C27), fatty hydroxy acids and diols. Long-chain compounds (fatty hydroxy acids with 30-34 carbon atoms or diols with 32 carbon atoms) are found in small amounts. Saculene is a cholesterol precursor triterpenoid, which has a branched molecule with 30 carbon atoms and double bonds in positions Δ2, Δ6, Δ10, Δ14, Δ18 and Δ22 [4]. It is not converted to cholesterol in sebocytes. It seems that the small percentage of cholesterol in sebum originates in the basement membrane of sebocytes, by destroying them [9, 10] and once it reaches the follicular duct, it is esterified [11].

Lipids in *stratum corneum* contain: about 50% ceramides, 25% cholesterol, ~15% free fatty acids, triglycerides and saculene, 2-5% cholesterol sulfate (cholesterol ester) [6, 12, 13]. Ceramides consist of sphingosine (an unsaturated amino alcohol with 18 carbon atoms) and a long-chain fatty acid, which can have as many as 34 carbon atoms. Free fatty acids have a chain with 14-24 carbon atoms dominated by saturated or monounsaturated acids (C18:1) [14]. Phospholipids occurs in small amounts, of only ~ 4%, but they are rich in oleic acid [13]. Human perspiration also contains proteins and antimicrobial peptides [14], sodium ions, calcium, magnesium, chlorine, potassium, lactates, urea, ammonia, bicarbonate and amino acids, some of which result from *metabolism* [14, 15].

This paper is aimed to show the unwanted effects of skin lipids as such and enhanced by fungal attack, to sound the alarm in order to give up harmful practices on old documents, and also to develop a compatible and environmentally friendly cleaning and preservation protocol.

Experimental Part

Materials

The materials that we analyzed come from a Register of Births, Marriages and Deaths of 1895, which is stored in one of the warehouses of Iași County Service of the National Archives. Due to its repeated use and leafing through with unprotected hands or, worse, by wetting one's fingers in one's mouth while in custody with the creator and holder of the document, the pages of this register suffered damage due to both improper handling and deposition of skin lipids on

the lower right corners, which, in time, have led to the degradation of both the support and the writing, especially under the influence of fungal attack. Some of these aspects are shown in figure 1.

Fig. 1. Images of areas with skin lipids that supported the onset of the biotic attack

The layer of lipids deposited on the surface of the cellulose support of the document, resulting from the two sources (saliva and skin lipids), has a negative influence on its state of preservation, not to mention its unsightly appearance. First, the fatty film containing lipids on the surface of human skin, lipids secreted by the sebaceous glands or resulting from the desquamation of the surface layer of keratinocytes in the palm, not only allows finger dirt to get stuck here, but also enhances the adhesion of atmospheric dust and smog, which, in time, through oxidative processes, become entangled or, through photochemical and thermal processes, become cornified. Thus, a cellulose substrate enriched with such products (lipids, proteins and carbohydrates from saliva or skin surfaces), along with their moisture content and hygroscopic water in the atmosphere, becomes an environment conducive to microorganism development. An extensive form of microorganism attack, which may be caused by such 'habits', is shown in Figure 2, in which a whole page has become the place where microorganisms grow and prosper.

Three specimens were sampled in this document marked as follows: **H**S – standard sample (the top of an inside page, without fingerprints or other marks), HLT (bottom of the page - the lower right corner used to browse through the document, with skin lipids) and HLTM (similar to HLT, yet with fungal attack and chromatic degradation).

The document has a cellulose support obtained by the Fourdinier process, with continuous casting. In other words, it is an industrial paper, in which wood pulp was used as

raw material, to which chemical delignification treatments were applied by alkaline leaching with sulfite, which is noticeable on its mere observation using magnifying instruments, and which will be later confirmed by SEM-EDX and μ-FTIR tests.

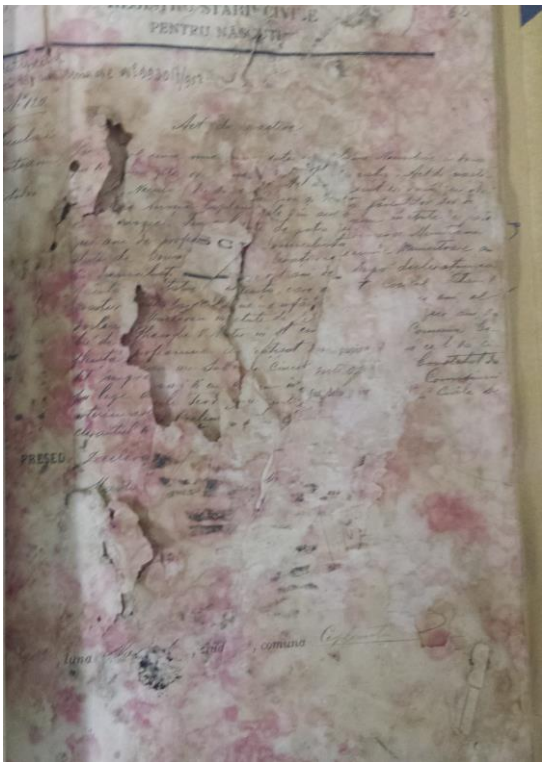

Fig. 2. Fungal attack inside the register taking up the entire page

Analysis Methods

In order to determine the chemical composition of the components of the cellulosic support and to evaluate their state of preservation, according to the analytical protocol, four testing methods were chosen involving several disciplinary techniques: optical microscopy (OM), scanning electron microscopy, coupled with X-ray diffraction (SEM-EDX), μ-FTIR spectrophotometry and thermogravimetric analysis, namely TG/TGA, and the differential thermal analysis, DTA. These methods enabled us to collect data about the morpho-structural characteristics, elemental composition and functional/molecular groups, with the vibration and deformation bands. TG/TGA thermogravimetric analysis showed a change in the mass of the sample depending on temperature and time, while the DTA differential thermal analysis aimed, based on thermal effects, to perform a qualitative analysis of the studied samples, based on the thermal loss behavior in time. To this end, the following techniques were used: for OM – a Carl Zeiss Axio Imager A1m device with magnifying power ranging between 50× and 200×, with an AXIOCAM camera attached to it and using specialized software; SEM-EDX analysis was carried out with a VEGA II LSH scanning electron microscope (SEM) manufactured by TESCAN in the Czech Republic, connected to a EDX QUANTAX QX2 detector manufactured by BRUKER/ROENTEC Germany, at 100...500× magnification, with BSE detector, 30kV accelerating voltage and working pressure below $1x10^{-2}$Pa; μ-FTIR – the spectra were determined using a FTIR TENSOR 27 spectrophotometer with OPUS software and connected to a HYPERION 1000 microscope, both pieces of equipment manufactured by Bruker Optic,

Germany, which for the purpose of our analysis, covered the 4000 - 600cm^{-1} spectrum range; differential thermal analysis was performed by means of a LINSEIS STA PT-1600 derivatograph made in Germany, at 600°C.

Results and Discussions

Analysis of morpho-structural characteristics using optical microscopy

We chose the most conclusive of a series of microphotographs taken at various magnifications with an optical microscope (Fig. 3), which enabled us to collect information about the structural morphology of the constituents of the cellulose support.

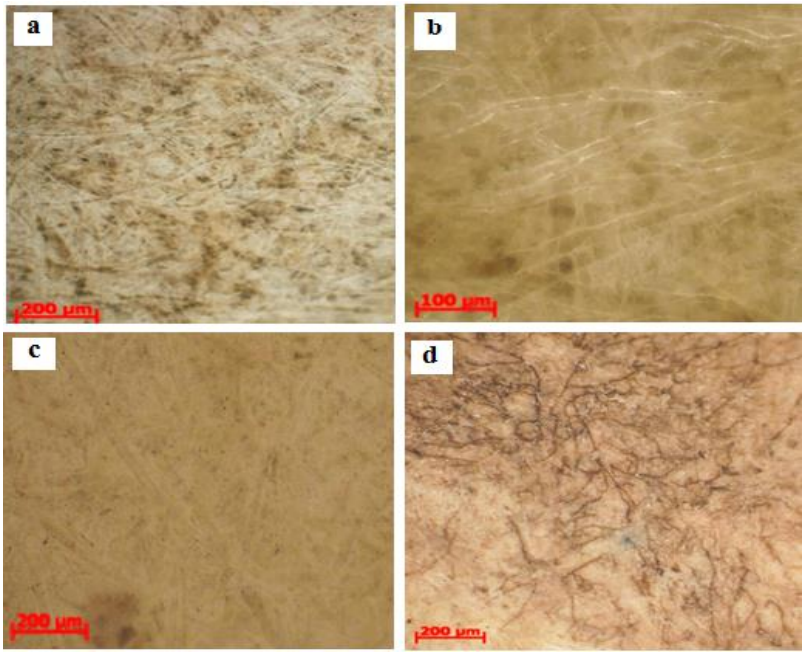

Fig. 3. OM microphotographs of paper samples:
a. HS – paper without skin surface lipids (100×); b - HS – paper without skin surface lipids (200×);
c. HLT – paper with skin surface lipids (100×); d - HLTM – paper with skin surface lipids and fungal attack (100×)

Figure 3a and b shows the microphotograph of the HS sample without skin surface lipids at 100× and 200× magnitudes, figure 3c shows the image of the HLT sample with skin surface lipids (100×), while figure 3d is the photograph of the HLTM sample with skin surface lipids and fungal attack (100×).

The analysis of the OM images reveals that the cellulose fibers of the HLT sample, which contains skin lipid film, and of the HLTM sample, with ongoing biotic attack, are more difficult to notice. Some micelles are very visible in the last sample, with fungal attack, in the form of rather well branched microscopic filament webs (hyphae), which originated in a few spores/germs. In this area, the document was damaged by enzymatic hydrolysis of cellulose fibers and chromatic degradations (the resulting pigments are brown, whitish and pink-purple, with the latter being predominant). The chromatic fungal attack does not greatly influence the resistance characteristics of the support, these being only color degradations, which raise major problems for restorers, since they cannot be easily removed. The chromatics of the pigments resulting from such microorganisms is influenced by a number of factors, such as: the composition of the environment, the nature of the microorganism growth substrate, the presence

and concentration of microelements, the pH of the substrate or the presence of other microorganisms cohabiting in the same area [1].

Electron microscopy analysis coupled with X-ray diffraction (SEM-EDX)

With the help of the SEM microscope, for the three samples, Microphotographs were taken of the three samples at two magnifications (100 × and 500 ×) using a SEM microscope, as shown in figure 4, which show a series of data related to the topography of surfaces and the morphology of fillers and cellulose fibers.

The SEM images reveal surface roughness, loose fibers and small legible areas with felted fibers in the standard sample and in the sample containing skin lipids (Fig. 4a/b and c/d), short cracks, areas with flaky fibers and crusts due to enzymatic degradation (Fig. 4e/f), all caused by fungal attack.

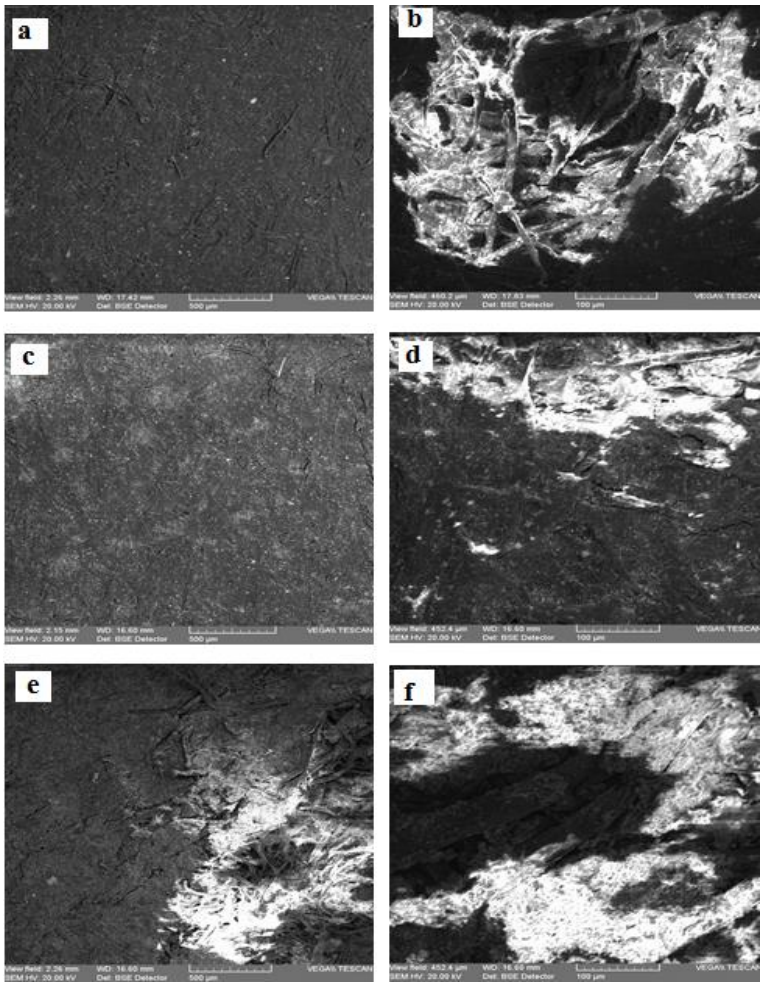

Fig. 4. SEM microphotographs of the analyzed samples:
a. HS - paper without skin surface lipids (100×, bse); b - **HS** - paper without skin surface lipids (500×, bse);
c - **HLT** - paper with skin surface lipids (100×, bse); d. **HLT** - paper with skin surface lipids (500×, bse);
e. HLTM - paper with skin surface lipids and fungal attack (100×, bse);
f. HLTM - paper with skin surface lipids and fungal attack (500×, bse);

All SEM microphotographs reveal small areas in which the cellulose fibers are clearly visible, for the remainder, due to the loss of binding capacity between fibers as nutrients from binders and fillers were consumed by fungi.

By corroborating SEM with visual analysis and OM microphotographs, small areas may be noticed on the analyzed surfaces where the effects of oxidative fouling and/or thermal/photochemical cornification of skin lipid deposits are visible, which allowed the welding (monolithization) of the fibers, which became frail, rigid/brittle.

We assessed the chemical composition of the document constituents by EDX carried out on all the three samples, which underwent, differentiated over time, a natural aging process and different degrees of yellowing and brittleness, especially due to fungal attack. These findings are very important, as they allow these data to be used in the development of preservation-restoration protocol [16-18].

Relying on the X-ray diffraction spectra (EDX) recorded for the entire surface of the SEM microphotograph, we assessed the elemental composition, in gravimetric percentages, of the three samples (Table 1).

Table 1. EDX Elemental composition (gravimetric percentages) determined by EDX

Sample	**Na**	**K**	**Mg**	**Ca**	**Al**	**Si**	**C**	**O**	**P**	**S**	**Cl**
HS	3.521	0.414	0.466	0.956	0.752	0.650	33.209	57.080		0.452	2.503
HLT	0.740	0.530	1.244	1.521	2.390	2.594	28.638	60.139	0.312	1.548	0.343
HLTM			0.865	0.629	1.597	1.183	32.204	62.568		0.954	

The HS sample, used as a standard, corresponds to a normal natural aging that took about 125 years with variations induced by contamination from manufacturing and storage in the warehouse and documentation room. On the other hand, the HLT sample, with skin lipid deposits, appears as discontinuous films with various thicknesses and colors in the affected areas, while the HLTM sample clearly reveals the effect of the fungal attack on surface texture and the arrangement of fibers and fillers. Elementary composition data allow drawing some conclusions:

- the presence, in the HS sample, of large amounts of sodium (3.521%) and chlorine (3.521%) shows that it originates in the delignification-bleaching processes (alkaline sulfite and hypochlorite solutions) and fillers; they occur in much smaller amounts in the HLT sample, due to dissolution under the influence of skin lipids;
- unlike the HS sample, the HLT sample shows a significant Mg, Ca, Al, Si and S increase and Na, C and Cl decrease, which may be accounted for by lipid contamination and hand and air dirt deposits;
- while it was initially due to the manufacturing processes, sulfur concentration tripled in the HLT sample (1.548%) compared to the HS sample (0.452%), due to the sulfur protides in skin surface lipids;
- phosphorus occurs only in the HLT sample (0.312%) and comes from skin phospholipids;
- the concentrations of all the elements show a decline in the HLTM sample, with ongoing fungal attack, compared to the HLT sample, with the exception of increasing carbon and oxygen, and of sodium, potassium, phosphorus and chlorine, which disappear completely, due to enzymatic degradation;
- unlike the HS and HLT samples, the HTLM sample completely misses sodium, potassium and chlorine due to enzymatic processes and dissolutions, followed by diffusions;
- the long HS fibers are not legible in the HLT and HLTM samples.

The analysis of the elemental composition reveals that a mixture consisting of: *calcium carbonate* ($CaCO_3$), *talc* ($3MgO{\cdot}4SiO_2{\cdot}H_2O$) and *kaolin* ($Al_2O_3{\cdot}2SiO_2{\cdot}H_2O$) was used as filler, and the gluing was achieved using rosin and alum [$KAl(SO_4)_2 \cdot 12H_2O$].

µ-*FTIR analysis*

In order to highlight the effect of skin lipids on the cellulose support of the document, including the biotic attack occurred following contamination, the three samples were analyzed by comparative means using µ-FTIR (Fig. 5).

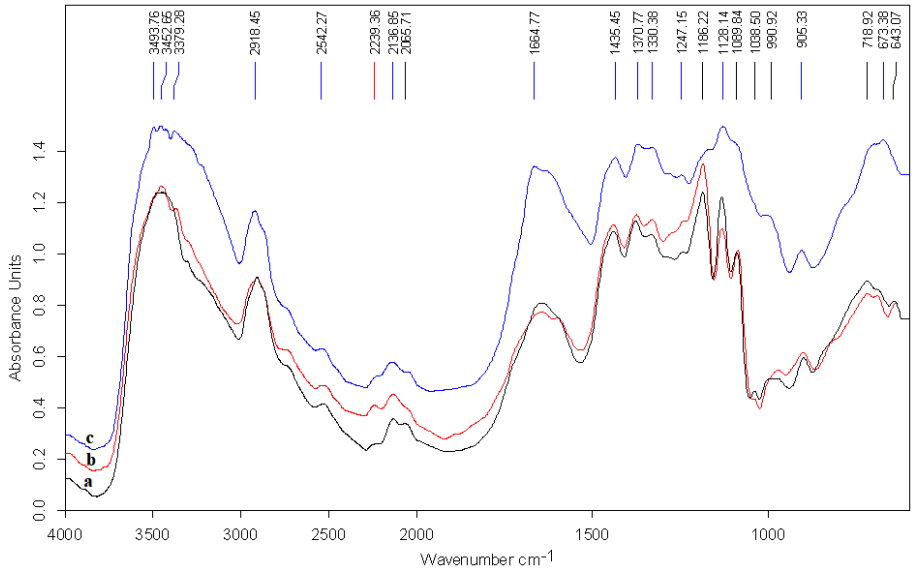

Fig. 5. FTIR spectra of the cellulose support: **a** – without skin surface lipids (HS); **b** – with skin surface lipids (HLT); **c** – with skin surface lipids and fungal attack (HLTM)

The FTIR spectra were recorded in reflection, within the 4000-600cm^{-1} range, at 4cm^{-1} resolution and consist of two regions:

- of 4000-1800cm^{-1} valence vibrations in which the peaks are characteristic of specific types of bonds;
- of 1800-600cm^{-1} deformation vibrations or fingerprints, in which the peaks are due to deformations of internal and external, symmetrical and antisymmetric molecular structures. The 1430-850cm^{-1} range has the highest complexity [19, 20].

The interpretation of the FTIR spectrum is done first by identifying the functional groups based on the valence vibrations (υ) and then by confirming them by the specific peaks of the deformation vibrations (δ).

Therefore, to begin with, we noted that the spectra of the three samples were somewhat similar, with the exception of a few differences, namely:

- compared to the HLT sample (with lipids) and to the HLTM sample (with lipids and fungal attack), the control HS sample (without lipids) has the size of a spectrum with lower intensity absorption bands;
- all three samples have similar spectrum sizes up to 1330cm^{-1}, having the same assignments for the peaks within this field (4000-1330cm^{-1});
- within the 1330 - 718cm^{-1} range, there are some differences between the appearances of the three samples; thus, the sample with biotic attack has higher absorption band intensities than the sample containing only lipids, which in turn has higher intensities than the sample without lipids;
- the valence vibrations specific to the –NH_2 bond, around the 3493cm^{-1} band, are blamed on the skin lipids and fungal attack, while those around the 3379cm^{-1} band, to the –OH bonds in the cellulose;

- the narrower 2918cm^{-1} band belongs to the –CH group in cellulose and lipids, while the HLT and HTLM ones are more intense;
- the narrow 2542, 1435 and 719cm^{-1} bands, of which the first is less intense, and the other two are very intense, are attributed to the carbonate ion;
- the sample with biotic attack and skin lipid deposits has a wide absorption band in the area of valence vibrations, with the three peaks (3493.76, 3452.66 and 3379.28cm^{-1}) and an intense peak in the area of the 1664.77cm^{-1} deformation bands, all attributed to the –OH and –H-O-H groups of cellulose microfibrils and binders, which shows the rate of degradation by enzymatic hydrolysis as a result of the disappearance of hydrogen bonds and the diminution of the leachate capacity of the binder;
- the 1439.90, 1370.77 and 1330.38cm^{-1} peaks may be attributed to calcium carbonate, and also to ketones, aldehydes and the –C-OH bond, the peaks within this range may also be attributed to the asymmetric deformation of the C-H bond in methyl groups (–CH_3), in hemicelluloses and lignin or deformation vibration of starch (–OH) groups;
- the 1274.12 and 1247.15cm^{-1} absorption band peaks (only in the case of the support sample with skin lipids) may also be attributed to the C-O groups;
- the 1186.22 and 1128.14cm^{-1} absorption band peaks are attributed to the asymmetric group C-O-C, which indicates the formation of intra- and intermolecular bonds, while the occurrence of absorption bands with 1089.84 and 1038.50cm^{-1} peaks demonstrates the disappearance of C-O groups;
- the 990.92 and 905.33cm^{-1} peaks may be attributed to the CO groups in starch;
- the 673.38cm^{-1} peak is attributed to the deformation vibration of the aromatic C-H groups in lignin, and also to the Al-O vibrations specific to aluminosilicates, plus the 643.07cm^{-1} peak, which occurs in the sample without skin surface lipids;
- the 1500-1200cm^{-1} range contains a series of distinct absorption bands, which are due to primary alcohol groups: CH_2-OH deformation vibrations at the following peak values: 1439.90, 1374.86, 1330.33 and 1185.44cm^{-1} and C-O and C-H bond deformation vibrations.

Based on the deformation vibrations of the –CH group from 1374.86 and from 2907.79cm^{-1}, the *degree of crystallinity (GC)* may be evaluated from their ratio, and the strength of hydrogen bonds may be determined using the ratio between the 1439.90cm^{-1} band and the 900.99 cm^{-1} bound hydrogen [21-23].

It is well known that the mechanical strength of cellulose fibers is influenced by the *degree of crystallinity*, which depends on the origin and type of pretreatment, and represents the ratio between the wave numbers corresponding to these peaks, specific to crystalline and amorphous areas [23, 24-27]. Also, the durability of paper cellulose fibers varies both depending on the *degree* or *index of crystallinity* (I_c) and of *lateral ordering* (G_{OL}), as well as on *the intensity of hydrogen bonds* (I_{legH}) and their *energy* (E_{legH}).

They are calculated according to the relative intensities of a band [28]; for instance, the hydroxyl group (-OH), to HS sample, with specific absorbance to both crystalline cellulose bands within the 1400 - 1200 cm^{-1} range, and amorphous bands, has the following ratio:

Degree or index of crystallinity, $I_c = A_{1376.77}/A_{2907.41} = 0.97$;

where: A is the absorbance of the (-OH) hydroxyl groups, specific to the crystalline cellulose and amorphous bands;

Degree of lateral ordering, $G_{OL} = A_{1439.16}/A_{899.15} = 1.92$;

Intensity of hydrogen bonds, $I_H = A_{3442.25}/A_{1332.80} = 44$ (the ratio between the intensities of the 3442.25cm^{-1} and 1332.80cm^{-1} absorption bands);

The value of the energy of hydrogen bonds are calculated according to the ratio = 1/1.6 x10^{-2}kcal^{-1} × $[(\nu_0 - \nu_{HS})/\nu_0]$, where ν_0 is the standard frequency of the free (–OH) groups, which is 3650cm^{-1}, while ν_{HS} is the frequency of the HS sample = 3442.25cm^{-1}.

Value of the energy of the hydrogen bonds $E_{leg\,H} = 3.56kcal$.

Table 2 shows the characteristics of the three samples, depending on the crystallinity of cellulose fibers.

Table 2. Calculation of the degree of crystallinity and lateral ordering, together with the intensity and energy of the hydrogen bonds, in the FTIR spectra of the three samples

Sample	Degree or index of crystallinity (I_c)	Degree of lateral ordering (G_{OL})	Intensity of hydrogen bonds (I_{legH})	Energy of hydrogen bonds (E_{legH}, kcal)
HS	$A_{1376.77}/A_{2907.41} = 0.97$	$A_{1439.16}/A_{899.15} = 1.92$	$A_{3442.25}/A_{1332.80} = 44$	3.56
HLT	$A_{1374.86}/A_{2907.79} = 0.87$	$A_{1439.90}/A_{900.99} = 1.35$	$A_{3453.93}/A_{1330.33} = 22$	3.36
HLTM	$A_{1370.77}A_{2918.45} = 1.27$	$A_{1435.45}/A_{905.33} = 1.57$	$A_{3452.65}/A_{1330.38} = 60$	2.68

According to the data in table 2, all samples have very low hydrogen bond energy, especially the one affected by fungal attack, which is much lower than the values of the other two samples. The crystallinity index in the three samples differs significantly, due to the inorganic components. At the same time, the differences in the energy of the hydrogen bonds indicate a strong entrainment of the OH groups in the formation of the H bonds consequently increasing the crystallinity of the samples. Also, the degree of lateral ordering is lower in the lipid-free sample, which is due to hydrolytic cleavage and natural aging of paper, as well as to the enzymatic hydrolytic cleavages present in the HLTM sample.

Thermogravimetric Analysis

Thermal analysis consists of a number of investigative methods that assess the thermal behavior of a substance or material, on the basis of which a number of its physical and chemical properties can be determined involving loss of material (TG) or thermal effects (DTA), which occur at certain temperature levels, by correlation with the heating time at a given rate, for instance 12°/min. The temperature parameter will be changed according to a preset schedule, the changes being recorded on an abscissa, while the physical properties changes will be recorded on the ordinate, the final result being a thermogram (graph that is created automatically) [29-31].

Here are the physical properties of substances that are temperature dependent and undergo changes according to a present schedule:

- mass, the change of which is measured by thermogravimetric analysis (TG);
- temperature and thermal effect at a given thermal threshold – by differential thermal analysis (DTA);

Thermal destruction studies of various materials are used to specify the thermal effects triggered at specific levels at which processes of removal/adsorption of volatile components, decomposition of different classes of macromolecular substances and cleavage of various types of bonds occur.

The following curves were recorded simultaneously to illustrate thermal decomposition by thermogravimetric methods using a Linseins, Germany derivatograph:

- T - temperature at any time;
- TG – sample mass at any time;
- DTA - temperature difference between the current sample and the Al_2O_3 standard sample.

This method highlights the stages of the thermal decomposition process, as well as the components of the samples that decompose (are destroyed) during this process.

The following determinations were made during each thermogravimetric stage: specific temperatures (process onset temperature - Ti, peak mass loss rate temperature - Tmax and final stage temperature - Tf); mass loss (Δm, %); thermal effect (DTA) and nature of processes.

The same three samples were considered, namely HS, HLT and HLTM, of which the following finely ground quantities were weighed on an analytical balance: 41.4mg HS, 41.2mg HLT and 42.5mg HLTM and inserted in the cylindrical ceramic boats.

Figures 6 show the TG/DTA curves (derivatograms) of the three samples.

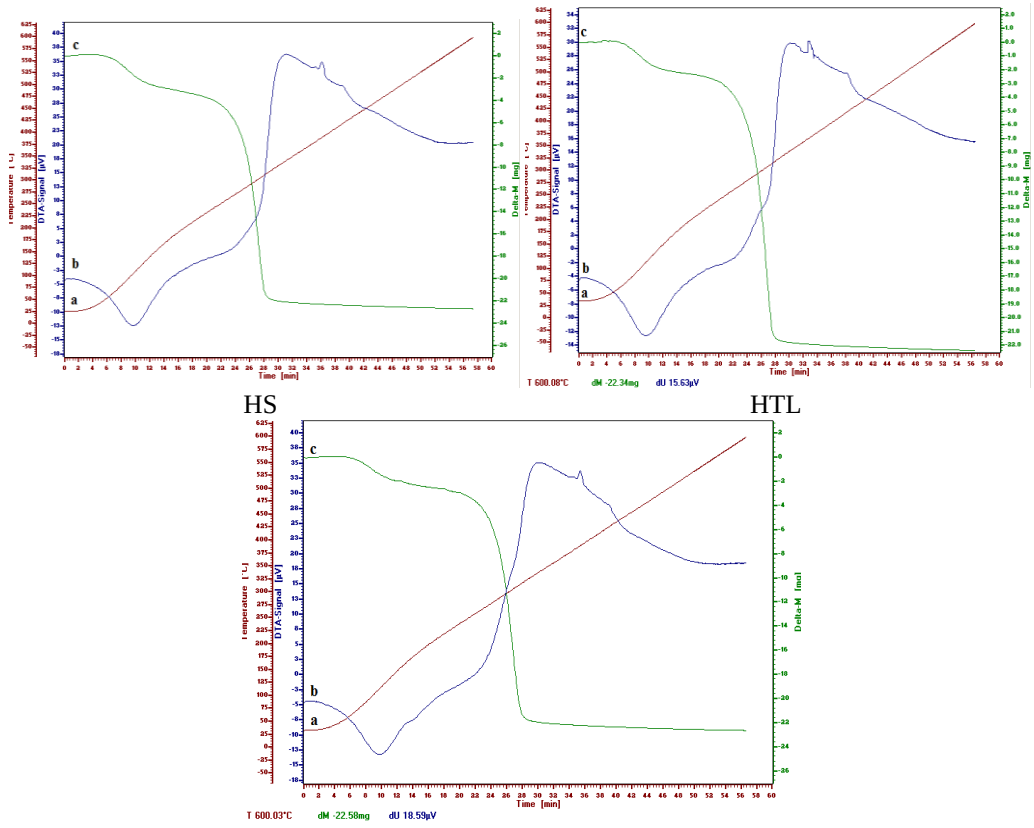

Fig. 6. Derivatograms of the three samples: a – temperature curve (red); b – DTA curve (blue); c – TG or mass loss Δm, % curve (green).

A brief analysis of the appearances of the three curves for the samples analyzed by thermal derivatography reveals the following (Fig. 7):

- the curves can be analyzed on the three clearly-defined stages of decomposition: 25 – 150°C; 150 – 330ºC and 330 –600°C;
- water and volatile component losses are recorded up to 100 - 150°C, as thermal decomposition actually begins above 150°C (read on the TG curve) and is conducted during the following two stages: the first ranging from 150 to 330°C, and the second ranging from 330 to 600°C.

In the three sequences, each component of a sample follows a distinct path of decomposition. As hemicelluloses are more susceptible to heat attack than cellulose, they decompose up to 300°C and generate carbonic residue that slowly loses mass, along with potential traces of lignin, at higher temperatures, i.e. above 300°C. For cellulose, starch and other macromolecular structures in the samples, the curves obviously follow the decomposition of carbohydrates, attest to a spontaneous development of catenary fragmentation reactions, radical within the 300-400°C range, revealed by the steep slope of the curves, and also of the other components. Fillers have a completely different evolution, as oxygenated salts (carbonates, sulphates, aluminosilicates, etc.) are more difficult to decompose and most of them end up in the ashes.

The amount of ashes in the three samples follows the sequences:

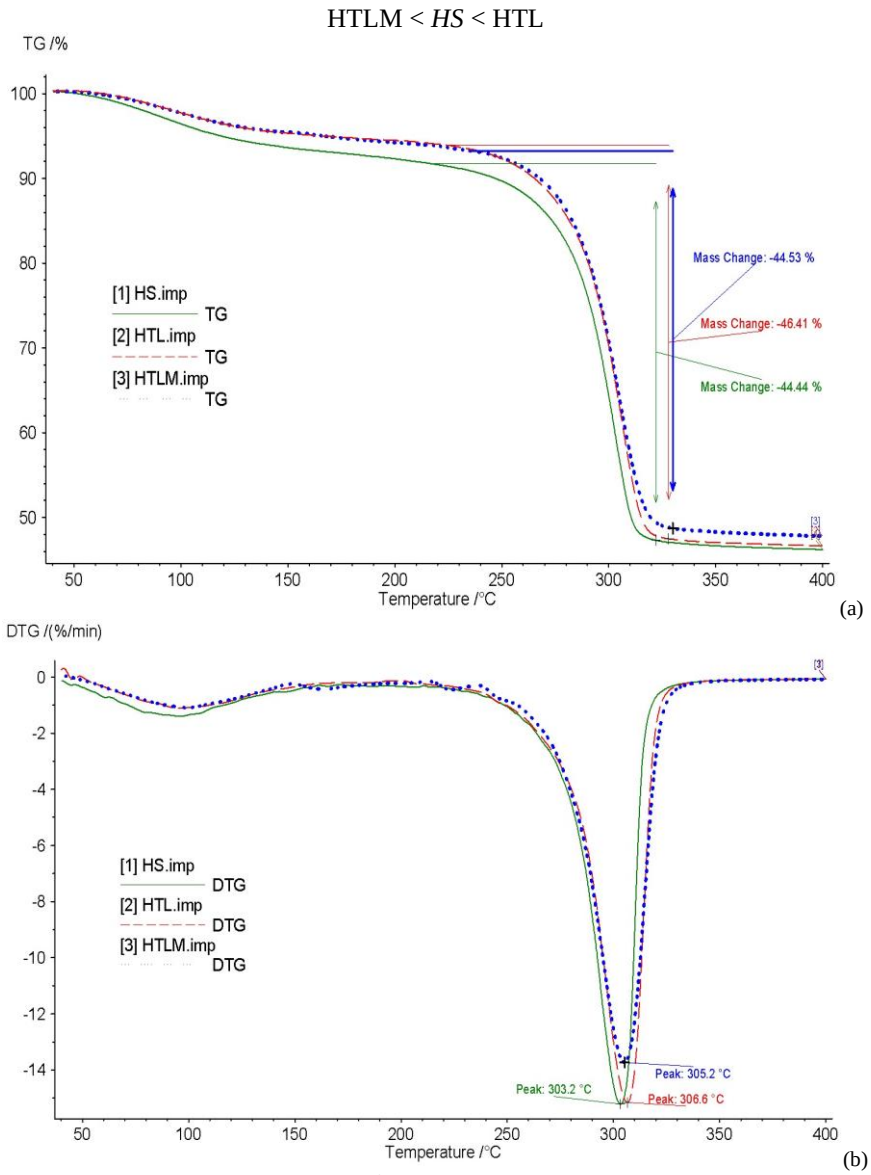

Fig. 7. TG (a) and DTG (b) curves for the second paper sample decomposition stage.

Cellulose, as a pure material, is clearly differentiated by its behavior during thermal destruction, falling in the range below 300°C, after which the reaction unfolds much more slowly, providing an increasingly significant thermal stability.

As lignin decomposes over a wider temperature range, its destruction mechanism accumulates slow processes of catenary recombination of cleaved fragments, subsequent crosslinking by condensation accompanied by gradual shortening of the length of macromolecules.

For the three samples analyzed by differential thermal analysis (Fig. 6), the specific temperatures of the three stages of thermal decomposition were determined, which are shown in table 2.

Table 2. Specific temperatures and mass loss for various decomposition stages of the HS, HTL and HTLM samples

Sample	Stage 1 20 - 150°C				Stage 2 **150-320**°C				Stage 3 **20-600**°C			
code	T_i	T_{max}	T_{fin}	**Δm(%)**	T_i	T_{max}	T_{fin}	**Δm(%)**	T_i	T_{max}	T_{fin}	**Δm(%)**
HS	25	95	150	5.4	217	303	322	44.4	322	450	600	54.1/48.7*
HTL	32	95	138	3.8	225	307	328	46.4	328	440	600	53.6/49.8*
HTLM	35	95	140	3.8	236	305	330	44.5	330	440	600	52.5/48.7*

* no moisture

The TG and DTG curves in Figure 7 and the thermogravimetric data in Table 2 reveals the differences in the thermal behavior of the studied paper samples. Up to 150°C, the paper samples with skin lipids had a mass loss of 3.8%, which is lower than in the plain paper sample, which lost only 5.4% of its mass. This indicates a lower humidity of the lipid-coated samples, which, due to their hydrophobic nature, reduce the absorption of water by the lining paper. The paper samples show a very slow mass loss, yet slightly higher in the lining paper, within the temperature range located after the removal of moisture but before the main decomposition stage (between 150 and ~ 220°C). The skin lipids most likely facilitated the transfer of small molecular compounds from the paper mass to its surface, from where they were more easily removed over the years.

The main decomposition stage begins differently for the three samples. Lining paper decomposes between 217 and 322°C, with a peak rate 303°C. Paper samples coated with skin lipids have their TG and DTG curves slightly shifted to higher temperatures, indicating their thermal stabilization. Thermal decomposition onset is slightly delayed for the sample that underwent fungal attack (HTLM), compared to the one without attack, yet the process, once started, unfolds faster, reaching its peak rate at 305°C, which is 2°C lower than the HTL sample. It seems that the fungal attack consumed some of the small molecular compounds in the paper (nutrients from the organic components and a small part of the inorganic ones), which decompose at lower temperatures in the support sample. The DTG curve of the HTLM sample shows slight inflections at ~ 165°C and between 225 and 245°C, due to its complex composition. The mass losses during the main decomposition stage are similar, i.e. ~ 45%, slightly higher in the paper sample coated with skin lipids but with no fungal attack. The final mass losses, at 600°C, are different, but if the water contribution is eliminated, a situation similar to the main decomposition stage is observed, with the HS and HTLM samples having similar mass losses (48.7%) and the HTL sample having a slightly higher mass loss (49.8%).

Conclusions

One of the very aggressive forms is related to browsing with no gloves and mask, not to mention that few archives and libraries have protection niches with controlled environment.

Many old documents on cellulosic media, after long periods of usage with unprotected hands and no mask, have on the corners of their pages, especially on the lower corners, a load of skin surface lipids, which over time have led to a series of evolutionary effects, mostly degradation.

The study of the behavior of skin lipid deposits required a detailed scientific research involving modern methods, such as: OM, SEM-EDX, μ-FTIR and differential thermal analysis (TG, DTA, DTG).

OM revealed that samples containing films of skin surface lipids and biotic attack have cellulose fibers more difficult to detect. In the fungal attack sample, the micelles in the form of well branched microscopic filament webs (hyphae) are very visible.

Degradation caused by enzymatic hydrolysis has the effect of cleavage of cellulose fibers, i.e. a high rate of degradation of the binder, which loses its leachable capacity. The chromatic fungal attack does not influence the mechanical characteristics of the support, but it

creates big problems for restorers, because they cannot be easily removed. The chromatics of the pigments resulting from such microorganisms is influenced by a number of factors, such as: the composition of the environment, the nature of the microorganism growth substrate, the presence and concentration of microelements, the pH of the substrate or the presence of other categories of microorganisms cohabiting in the same area.

The SEM images reveal surface roughness, loose fibers and small legible areas with felted fibers, short cracks, areas with flaky fibers and crusts due to enzymatic degradation, all caused by fungal attack.

The elemental EDX composition of the HS sample, used as standard, corresponds to a normal natural aging that took about 125 years with variations induced by contamination from manufacturing and storage in the warehouse and documentation room. On the other hand, the HLT sample, with skin lipid deposits, appears as discontinuous films with various thicknesses and colors in the affected areas, while the HLTM sample clearly reveals the effect of the fungal attack on surface texture and the arrangement of fibers and fillers.

In order to reveal the effect of skin surface lipids and biotic attack on the cellulosic support of the document, the three samples were compared using μ-FTIR, which only showed some small differences within the 1330 - 718cm^{-1} range, that of deformation vibrations for cellulose fibers, rosin-based binder, alum additive and fillers based on chalk powder, kaolin and talc.

The appearances of the three curves for the samples analyzed by thermal derivatography reveals the following:

- the curves showed easily detectable differences during the three clearly-defined stages of decomposition: 20 – 150°C; 150 – 320ºC and 320 – 600°C;
- the results of the thermal decomposition of the components of the three samples, classified according to the various temperature ranges, form the following sequence revealing the amount of resulting ashes: HTLM < HS < HTL;
- comparable results were achieved as concerns the three specific temperatures (T_i, T_{max} and T_f) and mass loss (Δm,%), where the differences between the standard sample and the sample with skin surface lipids, and the sample with skin surface lipids and fungal attack, respectively, were revealed;
- the data about the evolution of the T, DTA and TG curves (mass loss, Δm,%), and the TG and DTG curves, respectively, assessed during the second decomposition stage of the three paper samples are also comparable;

These studies reveal the aggressiveness of skin surface lipids and fungal attack, and the collected data are necessary for the development of experimental preservation and restoration protocols, and for taking urgent measures for the use of protection means (gloves and masks).

References

[1] F. Oprea, **Biology for the conservation and restoration of cultural heritage,** Ed. Maiko, Bucureşti, 2006.

[2] H.M. Sheu, S.C. Chao, T.W. Wong, J.Y.Y. Lee, J.C. Tsai, *Human skin surface lipid film: an ultrastructural study and interaction with corneocytes and intercellular lipid lamellae of the stratum corneum*, **British Journal of Dermatology, 140**(3), 1999, pp. 385-391.

[3] R. Michael-Jubeli, A. Tfayli, J. Bleton, A. Bailet-Guffroy, *Chemometric approach for investigating the skin surface lipids (SSLs) composition: influence of geographical localization*, **European Journal of Dermatology, 21,** 2011, pp. 63-71.

[4] Z.R. Huang, Y.K. Lin, J.Y. Fang, *Biological and Pharmacological Activities of Squalene and Related Compounds: Potential Uses in Cosmetic Dermatology*, **Molecules, 14**(1), 2009, pp. 540-554.

[5] E. Camera, M. Ludovici, M. Galante, J.L. Sinagra, M. Picardo, *Comprehensive analysis of the major lipid classes in sebum by rapid resolution high-performance liquid chromatography and electrospray mass spectrometry*, **Journal of Lipid Research, 51**(11), 2001, pp. 3377-3388. doi: 10.1194/jrl.D008391.
[6] C. De Luca, G. Valacchi, *Surface Lipids as Multifunctional Mediators of Skin Responses to Environmental Stimuli*, **Mediators of Inflammation, 10,** 2010, pp. 1-11.
[7] M. Picardo, M. Ottaviani, E. Camera, A. Mastrofrancesco, *Sebaceous glands lipids*, **Dermato-Endocrinology, 1**(2), 2009, pp. 68-71.
[8] T. Nakatsuji, M.C. Kao, L. Zhang, C.C. Zouboulis, R.L. Gallo, C.M. Huang, *Sebum Free Fatty Acids Enhance the Innate Immune Defense of Human Sebocytes by Upergulating b-Defensin-2 Expression*, **Journal of Investigative Dermatology, 130,** 2010, pp. 985-994.
[9] E. Camera, M. Ottaviani, M. Picardo, *Saqulene Chemistry and Biology*, **Lipids and Skin Health** (Editor: A. Pappas), Springer International Publisher, New York, 2015, p.185.
[10] P.W. Wertz, *Sebum Secretion and Acne*, **Acne and Its Therapy** (Editors: G.F. Webster and A.V. Rawlings), Taylor & Francis Group, Boca Raton, Florida, 2007.
[11] P. Agache, *Sebaceous Physiology*, **Measuring the Skin,** (Editors: P. Agache and P. Humbert), Springer-Verlag, Berlin, 2004.
[12] K.R. Feingold, *The role of epidermal lipids in cutaneous permeability barrier homeostasis*, **Journal of Lipid Research, 48,** 2007, pp. 2531-2546.
[13] M.A. Lampe, A.L. Burlingame, J. Whitney, M.L. Williams, B.E. Brown, E. Roitman, P.M. Elias, *Human stratum corneum lipids: characterization and regional variations*, **Journal of Lipid Research, 24**(2), 1983, pp. 120-130.
[14] J.A. Bouwstra, G.S. Gooris, *The Lipid Organisation in Human Stratum Corneum and Model Systems*, **The Open Dermatology Journal, 4**, 2010, pp. 10-13.
[15] K.A. Wilke, L. Martin, S.S.B. Terstegen, *A short history of sweat gland biology*, **International Journal of Cosmetic Science, 29,** 2007, pp. 169-179.
[16] M. Harker, H. Coulson, I. Fairweather, D. Taylor, C.A. Daykin, *Study of metabolite composition of eccrine sweat from healthy male and female human subjects by H NMR spectroscopy*, **Metabolomics, 2** (3), 2006, pp. 105-112.
[17] I. Sandu, I.C.A. Sandu, **Chemistry of Conservation and Restoration of Old Books, Vol. I, Chemistry of Processes and Study of Materials,** Alexandru Ioan Cuza University Publishing House, Iași, 1998;
[18] I.C.A. Sandu, C. Luca, I. Sandu, M. Pohontu, *Research regarding the soft wood support degradation evaluation in old paintings, using preparation layers. II. IR and FTIR Spectroscopy*, **Revista de Chimie**, **52(**7-8), 2001, pp. 409-419.
[19] D. Potolinca, I.C. Negru, V. Vasilache, C. Arsene, M. Paduraru, I. Sandu, *Forensic Expertise of the Paper Support of Counterfeit Documents*, **Materiale Plastice, 54**(1), 2017, pp. 186-189.
[20] N. Kruer-Zerhusen, B. Cantero-Tubilla, D.B. Wilson, *Characterization of cellulose crystallinity after enzymatic treatment using Fourier transform infrared spectroscopy (FTIR)*, **Cellulose**, 2017, DOI 10.1007/s10570-017-1542-0.
[21] P. Spiridon, I.C.A. Sandu, L. Nica, C.T. Iurcovschi, D.E. Colbu, I.C. Negru, V. Vasilache, R.A. Cristache, I. Sandu, *Archaeometric and Chemometric Studies Involved in the Authentication of Old Heritage Artefacts II. Old linden and poplar wood put into work*, **Revista de Chimie, 68**(10), 2017, pp. 2422-2430.
[22] S. Baccaro, M. Carewska, C. Casieri, A. Cemmi, A. Lepore, *Structure modifications and interaction with moisture in γ-irradiated pure cellulose by thermal analysis and infrared spectroscopy*, **Polymer Degradation and Stability**, **98**(10), 2013, pp. 2005-2010.
[23] M. Poletto, H.L. Ornaghi, A.J. Zattera, *Native Cellulose: Structure, Characterization and Thermal Properties*, **Journal of Materials Science,** 7(9), 2014, pp. 6105 – 6119.

[24] V.I. Popa, I. Spiridon, N. Anghel, **Biotechnological Processes in the Pulp and Paper Industry,** Ed. Media-Tech, Iași, 2001.
[25] I.C.A. Sandu, C. Luca, I Sandu, P. Atyim, *Research regarding the soft wood support degradation evaluation in old paintings, using preparation layers. 1. Chemical composition and technical analysis*, **Revista de Chimie, 52** (1-2), 2001, pp 46-52.
[26 P. Spiridon, I.C.A. Sandu, L. Nica, V. Vasilache, I. Sandu, *Archaeometric and Chemometric Studies Involved in the Authentication of Old Heritage Artefacts I. Contributions of the Iasi school of Conservation Science,* **Revista de Chimie, 68**(9), 2017, pp. 2018-2027.
[27] R.A. Cristache, I.C.A. Sandu, A.M. Budu, V. Vasilache, V, I. Sandu, *Multi-analytical Study of an Ancient Icon on Wooden Panel,* **Revista de Chimie, 66**(3), 2015, pp. 348-352.
[28] D. Fengel, *Characteristics of cellulose by deconvoluting the OH valency range in FTIR spectra*, **Holzforschung**, **46**(4), 1992, pp. 283-288. DOI: https://doi.org/10.1515/hfsg.1992.46.4.283
[29] J. Haines, **Thermal Methods of Analysis. Principles, Applications and Problems,** Blakie Academic & Professional, London, 1995;
[30] I.C.A. Sandu, M. Brebu, C. Luca, I. Sandu, C. Vasile, *Thermogravimetric study on the ageing of lime wood supports of old paintings*, **Polymer Degradation and Stability, 80**(1), 2003, pp. 83-91. DOI: 10.1016/S0141-3910(02)00386-5
[31] C. Luca, I.C.A. Sandu, *Research on the influence the solvents used in active preservation processes have upon old paintings supports, with preparation layer. I. Chemical composition, thermal analysis and IR study of the old, soil wood supports,* **Revista de Chimie, 49**(9), 1998, pp. 638-645.

Received: January 28, 2020
Accepted: August 28, 2020